Electronic band properties of $CaSr_2Bi_2Cu_2O_8$

L. F. Mattheiss and D. R. Hamann
AT&T Bell Laboratories, Murray Hill, New Jersey 07974
(Received 18 March 1988)

The electronic structure of body-centered tetragonal $CaSr_2Bi_2Cu_2O_8$, an undistorted stoichiometric prototype of the latest high-T_c superconducting cuprate, has been calculated with the use of the linear augmented-plane-wave method. The overall results are similar to those of the earlier cuprates, exhibiting band characteristics that are strongly two dimensional. The new compound features pairs of conducting BiO and CuO_2 planes in which the lowest pair of antibonding Bi($6p$)-O($2p$) bands are slightly (~4%) occupied and the corresponding pair of planar Cu($3d$)-O($2p$) bands are less than half filled (~46%).

The report[1] of high-temperature superconductivity in the Ca-Sr-Bi-Cu-O system, with onsets as high as ~110 K, has stimulated many workers to confirm these results and to determine the composition[2,3] and crystal structure[4-9] of the superconducting phase. It is generally agreed that the superconducting phase has a composition that is close to $CaSr_2Bi_2Cu_2O_8$; its reported structure is a complicated orthorhombic one which contains an incommensurate superlattice ($\sim 4.8b$) within the basal plane where $a \approx b$. The proposed structure is closely related to the so-called Aurivillius phases.[10]

Neglecting the superlattice effects and the small orthorhombic distortion, the essential features of the observed orthorhombic structure can be represented in terms of a prototype body-centered-tetragonal (bct) phase [space group $I4/mmm$, with $a = 3.83$ Å and $c = 30.89$ Å (Ref. 5)] which contains a single $CaSr_2Bi_2Cu_2O_8$ formula unit per primitive cell. This slightly idealized model structure consists of successive layers of BiO-SrO-CuO_2-Ca-CuO_2-SrO-BiO that repeat along the c axis in such a way that the registry of neighboring cells is shifted in the basal plane by $(a/2,a/2)$ because of the body-centering translation. The structure contains pairs of CuO_2 layers which are reminiscent of those in the La_2CuO_4 (2:1:4) and $YBa_2Cu_3O_7$ (1:2:3) phases. The analogy with the 1:2:3 compound suggests that the CuO_3 chains are replaced by a pair of BiO layers in the present material.

The important question that is addressed here concerns the effect of these BiO double layers on the planar Cu $d(x^2-y^2)$-O $p(x,y)$ bands that are nearly half-filled in the 2:1:4 and 1:2:3 compounds[11,12] since these are generally believed to provide the superconducting carriers in these materials. Based on previous calculations[13] for the perovskite-type $BaPb_{1-x}Bi_xO_3$ alloy system, one might expect the Bi $6s$ electrons to be chemically active, forming partially filled Bi($6s$)-O($2p$) conduction bands. However, an analysis of the nearest-neighbor Bi–O bond distances in the $CaSr_2Bi_2Cu_2O_8$ structure[5] yields values (~2.7 Å) that are significantly (~25%) larger than those found in the $BaPb_{1-x}Bi_xO_3$ system. This suggests that the formal valence of Bi in the present compound may be closer to 3+ than 4+, in which case the $6s$ states would be filled and the $6p$ bands might be chemically active.

The CuO_2 layers are widely believed to display strong correlation effects in all the high-T_c materials, leaving the applicability of the local-density-functional approximation employed here open to question. Indeed, in the limit that the uppermost band of the CuO_2 layer is exactly half filled (as in stoichiometric La_2CuO_4), the material is an antiferromagnetic insulator, and a Mott-Hubbard description is undoubtedly necessary. Nevertheless, the charge densities and the overall interlayer electrostatic potential should be given properly by the local-density method. In particular, the bands of the BiO layer should not be influenced by strong correlation effects, and their position and filling should be properly described by this scheme. In addition, local-density results provide calibration points for model Hamiltonians to be used in strong-correlation calculations. These models should have their parameters set to reproduce the present bands when treated in a Hartree-Fock approximation.

The self-consistent band structure for bct $CaSr_2Bi_2Cu_2O_8$ has been calculated in the local-density approximation with the use of the scalar-relativistic version[14] of the linear augmented-plane-wave (LAPW) method. The implementation imposes no shape approximations on either the charge density or the potential. The LAPW basis has included plane waves with energies up to 11.25 Ry (~1000 LAPW's) and spherical-harmonic cutoffs with either $l = 8$ (Ca, Sr, Bi), $l = 6$ (Cu), or $l = 5$ (O), depending on the size of the muffin-tin radii. The charge density and potential are expanded using ~10000 plane waves (55 Ry) in the interstitial region and by means of lattice-harmonic expansions ($l = 6$ for Ca, Sr, Bi, Cu and $l = 4$ for O) within the muffin-tin spheres. A ten-point **k** sample in the $\frac{1}{16}$ irreducible wedge was used to carry out the Brillouin-zone integrations. Exchange and correlation effects have been included with the use of the Wigner interpolation formula.[15]

The present calculations are based on the structure derived from the x-ray diffraction results of Ref. 5. A detailed listing of the internal position coordinates is given elsewhere.[16] The atomic Ca($4s^2$), Sr($4p^6 5s^2$), Bi($6s^2 6p^3$), Cu($3d^{10} 4s^1$), and O($2s^2 2p^4$) states are treated as valence-band electrons, whereas the more tightly bound corelike states are handled using a frozen-core approximation.[14]

The present LAPW results for bct $CaSr_2Bi_2Cu_2O_8$ are

plotted along symmetry lines in the basal plane of the Brillouin zone in Fig. 1. The occupied states consist primarily of the 34 bands that evolve from the Cu($3d$)-O($2p$) manifold. The unoccupied bands have predominant Bi($6p$) character. The overall valence bandwidth ($\sim$6.5 eV) is slightly smaller than that ($\sim$7.0 eV) obtained[16] using the linear muffin-tin-orbital method with the atomic-sphere approximation (LMTO-ASA). We have carried out extensive tests of the convergence of the hybridized Cu($3d$)-O($2p$) bands in a model CuO structure and established that the present results are converged to within 0.2 eV. A similar valence bandwidth has also been obtained in an independent LAPW study[17] of this material. As we anticipated on the basis of the Bi—O bond lengths, the Bi $6s$ bands are fully occupied and lie between -10 and -11 eV, well below the bands shown in Fig. 1. Other low-lying valence bands include the Sr $4p$ (-14.5 eV) and O $2s$ (-16 to -18 eV) levels.

The $CaSr_2Bi_2Cu_2O_8$ bands are strongly two dimensional, exhibiting minimal ($\sim$0.1 eV) dispersion along the c axis. Two distinct types of subbands intersect the Fermi level. These are identified by means of square and triangular symbols, respectively. The squares correspond to a pair of nearly degenerate antibonding Cu $d(x^2-y^2)$-O(1) $p(x,y)$ subbands which are analogous to those found in previous calculations[11,12] for the 2:1:4 and 1:2:3 superconductors. These subbands have their maximum energy at X, the Brillouin-zone boundary along [110]. The triangles denote a second set of subbands that arise from the Bi-O(2) planes. As shown in Fig. 1, the lowest portions of these subbands are occupied at D, near the [100] boundary. These represent antibonding combinations of Bi $p(x,y)$-O(2) $p(x,y)$ orbitals. The corresponding bonding combinations of these Cu($3d$)-O(1)($2p$) and Bi($6p$)-O(2)($2p$) states are also identified by the same symbols in the lower portions of the 34-band Cu($3d$)-O($2p$) manifold.

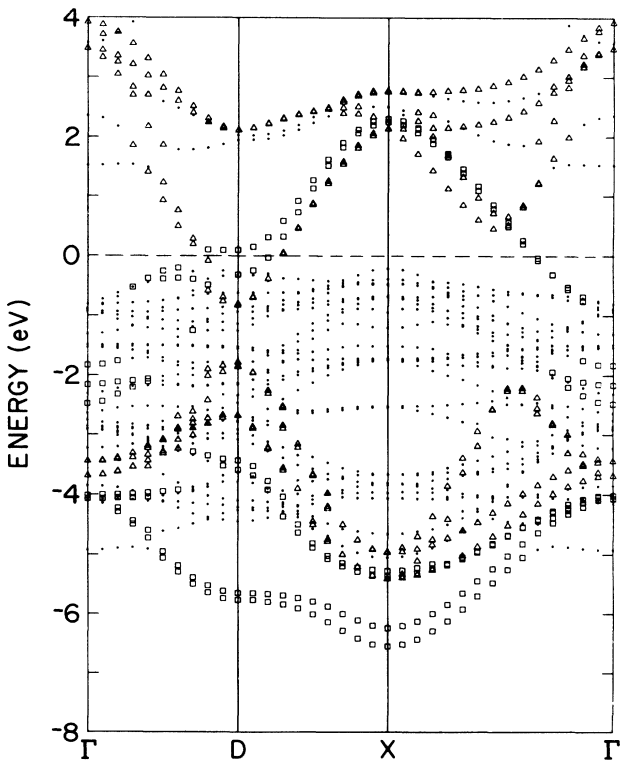

FIG. 1. Energy-band results for $CaSr_2Bi_2Cu_2O_8$ along symmetry lines in the basal plane of the bct Brillouin zone, where $D=(1,0,0)$ and $X=(1,1,0)$ in units of π/a. Those bands indicated by squares (triangles) have at least 30% (20%) Cu $d(x^2-y^2)$-O(1) $p(x,y)$ [Bi $p(x,y)$-O(2) $p(x,y)$] orbital weight within the corresponding muffin-tin spheres, where O(1) and O(2) denote oxygens in the Cu and Bi planes, respectively.

The general dispersion characteristics of these two distinct types of subbands can be understood in terms of simple tight-binding models.[11,16] For the Cu $d(x^2-y^2)$-O(1) $p(x,y)$ states, a simple two-parameter tight-binding model with degenerate Cu($3d$) and O($2p$) orbital energies and nearest-neighbor hopping terms[16] ($E_p=E_d=-2.6$ eV, $\sqrt{3}pd\sigma/2=-1.6$ eV) is sufficient. A detailed analysis shows[16] that a more elaborate tight-binding model is required in order to represent the characteristic features exhibited by the Bi $p(x,y)$-O(2) $p(x,y)$ subbands. In particular, this analysis shows that the Bi($6p$) orbital energy is above E_F and that both Bi-Bi and Bi-O hopping integrals are required to replicate the slightly occupied pair of antibonding Bi($6p$)-O(2)($2p$) subbands at D.

The three bands that intersect E_F in Fig. 1 provide a relatively low total carrier density ($\sim 8.8\times10^{21}$ cm^{-3}), with about 4×10^{21} carriers/cm^3 in each of the CuO_2 planes and 0.4×10^{21} carriers/cm^3 in each BiO plane. The remaining "background" bands in the range 0 to -6 eV in Fig. 1 include π-bonding and nonbonding Cu($3d$) and O($2p$) bands. One easily identified difference between our LAPW bands and the LMTO-ASA results[16] is the presence of a pair of flat bands at -2.5 eV in Fig. 1 that occur in the middle of a gap extending from -1.7 to -3.6 eV at X. We have identified these as nonbonding O(2) $p(z)$ orbitals, and believe that the tetragonal anisotropy of the electronic potential, which is spherically averaged in the ASA, is responsible for this discrepancy.

The LAPW valence charge density for these materials is illustrated by means of the contour plots in Fig. 2. The strongest bonding occurs along the nearest-neighbor Cu—O(1) bond directions, as shown in Fig. 2(a). Note the weaker coupling between the pair of Cu-O(1) planes and the Sr-O(3) planes. The nearest-neighbor Bi-O(2) and Bi-O(3) bonding is comparable, as shown in Fig. 2(c). The central Ca layer also shows extremely low density, consistent with the apparent isolation of the two CuO_2 layers that is reflected in the near-degeneracy of the pairs of CuO_2 bands in Fig. 1. Because of the bct Bravais lattice, the charge-density results in the lower left of Fig. 2(c) are displaced to the right by half the panel width in order to describe the repetition in the adjoining cell along the c axis. The "crescent moon" of charge above the top Bi is in fact directed towards a translated O(2) in the next cell. For the central (100) plane in Fig. 2(a), the corresponding repetition along c involves a similar matching of the central and noncentral panels in Figs. 2(a) and 2(b), respectively.

The density-of-states results that are obtained from the

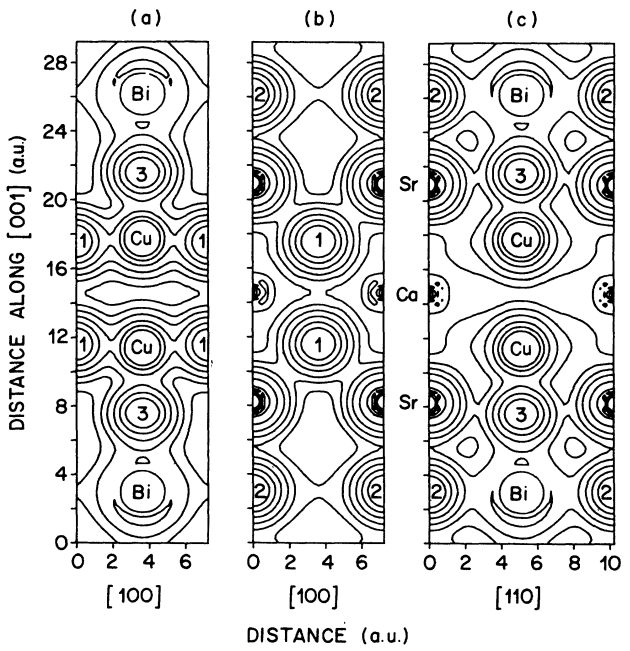

FIG. 2. Charge-density contours on the (a) central (100) plane, (b) noncentral (100) face, and (c) central (110) plane of the primitive bct $CaSr_2Bi_2Cu_2O_8$ structure. The oxygens in the Cu, Bi, and Sr planes are labeled 1, 2, and 3, respectively. The innermost Cu and O contour values are 0.46 electrons/(a.u.) (Ref. 3). The contour increments are spaced logarithmically, three to the decade (0.46, 0.22, 0.1, etc.).

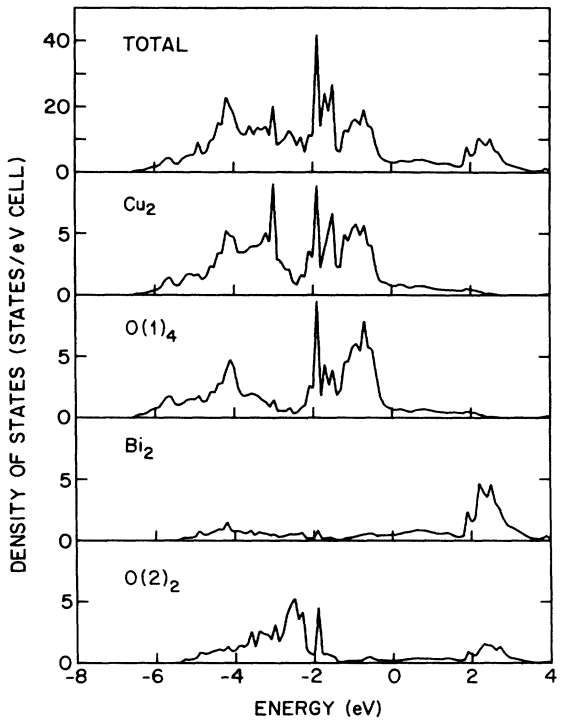

FIG. 3. Total and muffin-tin projected density-of-states results for $CaSr_2Bi_2Cu_2O_8$. The projected results focus on the conducting Cu-O(1) and Bi-O(2) planes.

present LAPW calculations are shown in Fig. 3. As in the case of the 2:1:4 and 1:2:3 cuprates,[11,12] the total density of states at E_F is relatively low ($\sim$3.0 states/eV cell). Similar values have been obtained from independent LMTO-ASA (Ref. 16) and LAPW (Ref. 17) calculations. The near-degeneracy of the Cu($3d$) and O(1)($2p$) orbital energies (~ -2 eV) is apparent visually from the center of gravity of the Cu_2 and $O(1)_4$ projected density-of-states results. A similar comparison of the Bi_2 and $O(2)_2$ results demonstrates that the Bi $6p$ weight is predominantly above E_F while that of O(2) $2p$ is below, which is consistent with the simple tight-binding interpretation discussed above.

Since the mechanism of high-T_c superconductivity in the cuprates is not yet understood, we can only speculate on the relationship of the special features of the electronic structure of the present material to this phenomenon. It may be that the only role played by the BiO layers is to contribute to the doping of carriers into the CuO_2 layers, and that the difference between the 2:1:4 40-K compound and the two 90-K materials is related only to doping effects and small changes in the parameters describing the individual CuO_2 layers. Alternatively, one could argue in light of the present results that there is a common feature present in the electronic structure of the $\sim$90-K materials that is absent in the 40-K family. The 2:1:4 family has metallic CuO_2 planes separated by insulating LaO layers, while the 1:2:3 compound and the present material have a metallic layer or bilayer in intimate contact with two CuO_2 layers.[11,12] While the properties of the CuO chains in the 1:2:3 phase are quite different from those of the present $(BiO)_2$ bilayers in terms of dimensionality and correlation effects, both provide a source of low-energy electronic excitations which could play an active role in boosting T_c.

The most recently announced high-T_c material, which appears to be related to $CaSr_2Bi_2Cu_2O_8$ by the substitution of Tl for Bi,[18] should provide yet another variant of interlayer electronic structure. We expect that the "triangle" Bi-O band complex in Fig. 1 will move more or less rigidly up across the other bands so that four electrons will be lost primarily from the Tl layers to maintain approximately the same electrostatic balance as achieved here. This should put Tl $p(x,y)$-O(2) $p(x,y)$ σ-bonding bands at the Fermi level. As the data base of high-T_c cuprates expands, it is clear that the systematics of these potentially active interlayers must be understood as one piece of the complex puzzle.

[1]H. Maeda, Y. Tanaka, M. Fukutomi, and T. Asano, Jpn. J. Appl. Phys. Lett. **27**, L209 (1988).
[2]C. W. Chu *et al.*, Phys. Rev. Lett. **60**, 941 (1988).
[3]R. M. Hazen *et al.*, Phys. Rev. Lett. **60**, 1174 (1988).
[4]M. A. Subramanian *et al.*, Science **239**, 1015 (1988).
[5]S. A. Sunshine *et al.*, Phys. Rev. B **38**, 893 (1988).
[6]J. M. Tarascon *et al.*, Phys. Rev. B **37**, 9382 (1988).
[7]H. W. Zandbergen *et al.*, Nature **332**, 620 (1988).

[8]J. P. Zhang *et al.* (unpublished).
[9]P. Bordet *et al.* (unpublished).
[10]B. Aurivillius, Ark. Kemi **1**, 463 (1950).
[11]L. F. Mattheiss, Phys. Rev. Lett. **58**, 1028 (1987); L. F. Mattheiss and D. R. Hamann, Solid State Commun. **63**, 395 (1987).
[12]J. Yu, A. J. Freeman, and J.-H. Xu, Phys. Rev. Lett. **58**, 1035 (1987); S. Massidda, J. Yu, A. J. Freeman, and D. D. Koelling, Phys. Lett. A **122**, 198 (1987).
[13]L. F. Mattheiss and D. R. Hamann, Phys. Rev. B **28**, 4227 (1983).
[14]L. F. Mattheiss and D. R. Hamann, Phys. Rev. B **33**, 823 (1986).
[15]E. Wigner, Phys. Rev. **46**, 1002 (1934).
[16]M. S. Hybertsen and L. F. Mattheiss, Phys. Rev. Lett. **60**, 1661 (1988).
[17]H. Krakauer and W. E. Pickett, Phys. Rev. Lett. **60**, 1665 (1988).
[18]Z. Z. Sheng *et al.*, Phys. Rev. Lett. **60**, 937 (1988).